2 MINERνA Physics Drivers

2.1 Quasi-Elastics

2.2 Resonance Production

2.3 Coherent Pion Production

MINERνA's high rates, range of nuclear targets, fine granularity, strong pattern recognition capabilities, and good electromagnetic calorimetry will make it possible to study charged- and neutral-current coherent neutrino-nucleus scattering with unprecedented precision. In this section we will briefly review the capabilities of the detector in this area focusing on the requirements placed on the detector design.

2.3.1 Introduction

Coherent neutrino-nucleus reactions, in which the neutrino scatters coherently from an entire nucleus with small energy transfer, leave a relatively clean experimental signature and have been studied in both charged-current ($\nu_\mu + A \rightarrow \mu^- + \pi^+$) and neutral-current ($\nu_\mu + A \rightarrow \nu + \pi^0$) interactions of neutrinos and anti-neutrinos. Although the coherent interaction rates are typically an order of magnitude or more lower than other single-pion production mechanisms, the distinct kinematic characteristics of these events allow them to be cleanly identified. Because the outgoing pion generally follows the incoming neutrino direction, this reaction is an important background to searches for $\nu_\mu \rightarrow \nu_e$ oscillation, as these events can easily mimic the oscillation signature of a single energetic electron shower.

A unique strength of the experiment is the ability to study both neutral and charged current channels from a variety of nuclear materials ranging from carbon to lead in the same experiment. Kinematic predictions from models can be explored in the charged current sample where the kinematics are fully reconstructed. The comparison of angular and energy distributions for produced pions in neutral and charged-current events will provide useful constraints on the various models, several of which predict CC/NC ratios differing by around 20% [1, 2]. A systematic comparison of charged- and neutral-current coherent production is currently a topic of considerable interest. While data on single π^0 production from the K2K and miniBoone experiments are in reasonable agreement with predictions [3, 4], a search for coherent CC production in the K2K experiment found only 7.6 ± 50.4 events where 470 were expected. This large difference between NC and CC production has been the subject of considerable theoretical work [5, 6, 7, 8] and could also account for the depletion at low Q^2 of inelastic events as compared with Monte Carlo predictions [9, 10].

2.3.2 Charged-current cross-section

The kinematics of coherent scattering are quite distinct compared to the more common deep-inelastic and resonant interactions. Because the coherence condition requires that the nucleus remain intact, low-energy transfers to the nuclear system, $|t|$, are needed. Events are generally defined as coherent by making cuts on the number of prongs emerging from the event vertex followed by an examination of the t distribution, where t is approximated by:

$$-|t| = -(q - p_\pi)^2 = (\Sigma_i(E_i - p_i^{||}))^2 - (\Sigma_i(p_i^{\perp}))^2 \quad (1)$$

With its excellent tracking capabilities, MINERνA's inner detector can measure this kinematic variable well.

To quantify MINERνA's ability to measure the charged-current coherent cross-section, a Monte Carlo study was carried out using the GEANT detector simulation described in Section **??**. Analysis cuts were tuned on a sample of coherent interactions corresponding to a four-year run with the three-ton fiducial volume. Events were generated according to the appropriate mix of low and medium energy beams. This study used the Rein-Seghal [1] model of coherent production, as implemented in NEUGEN3. A low-energy beam sample containing all reaction channels was used for background determination. Based on published bubble chamber analyses, charged-current reactions should be the largest background contributor, in particular quasi-elastic and Δ-production reactions where the baryon is mis-identified as a pion or not observed. To isolate a sample of coherent interactions, a series of cuts are placed on event topology and kinematics. The detector response is parametrized based on measurement smearing of 0.5^o angular resolution for reconstruction of muon and pion tracks, $18\%/\sqrt{E_{had}}$ hadronic energy resolution, and 10% muon energy resolution.

Topological cuts An initial set of topological cuts are applied to isolate a sample of events which contain only a muon and charged pion. These cuts are based on the hit-level and truth information as provided by the GEANT simulation.

1. **2 Charged Tracks:** The event is required to have 2 visible charged tracks emerging from the event vertex. A track is assumed to be visible if it produces at least 8 hit strips in the fully active region of the detector which are due to this track alone.

2. **Track Identification:** The two tracks must be identified as a muon and pion. The muon track is taken to be the most energetic track in the event which does not undergo hadronic interactions. The pion track is identified by the presence of a hadronic interaction. The pion track is required not to have ionization characteristic of a stopping proton (which is assumed can be identified 95% of the time).

3. **π^0/neutron Energy:** Because MINERνA is nearly hermetic we also assume that neutral particles will produce visible activity which can be associated with the event and used to exclude it. Events with more than 500 MeV of neutral energy (π^0 or neutron) produced in the initial neutrino interaction are rejected.

4. **Track Separation:** To make good measurements of the two tracks, the interaction point of the pion must be more than 30 cm from the primary vertex, and at this interaction point, at least 4 must strips separate the two tracks in at least one view.

Kinematic cuts Because coherent and background processes have very different kinematics, cuts on kinematic variables are effective in isolating the final sample. Kinematic quantities are estimated from the smeared measurements of muon energy, pion energy, and muon angle measurement under the assumption that the event in question is CC-coherent. Kinematic cuts are as follows:

1. **$x_{Bj} < 0.2$:** Requiring Bjorken-x (as reconstructed from the observed pion and muon 4-momenta) less than 0.2 eliminates much of the background from quasi-elastic reactions with $x_{Bj} \sim 1$.

2. $\boldsymbol{t < 0.2}$ **(GeV/c)^2:** The most powerful variable for the identification of coherent events is the square of the 4-momentum transfer to the nucleus. Equation 1 relating t to the observed particles in the event is used as the estimator of this quantity.

3. $\boldsymbol{p_\pi > 600}$ **MeV:** Requiring $p_\pi > 0.6$ GeV effectively eliminates background from Δ excitation, which tends to produce lower energy pions.

Signal and background distributions for several of the important cut variables are shown in Figure 2. The relative normalizations of the two distributions in the initial plot is arbitrary; subsequent plots show the effect of the applied cuts.

Applying this set of cuts to our signal sample (25,000 events) we find that 7400 signal events pass all cuts, which gives an overall efficiency of 30%. The expected purity of the sample is 67$\pm$3%, where the error bar is the statistical error on the Monte Carlo sample used for the study. We note that in this analysis other important variables for background rejection, related to associated activity around the vertex, were not used. Figure 2 shows the expected precision of the MINERνA measurement as a function of neutrino energy. Here we have only included the statistical error on the signal and assumed that the measured value is that predicted by Rein-Seghal. No attempt has been made to quantify the systematic errors on this measurement other than that resulting from the background subtraction. Previous measurements of the coherent cross-section were statistics limited.

2.3.3 Detector requirements

Figure 3 shows the efficiency and purity of the CC-coherent selection as a function of the assumptions about the measurement resolution of the detector. This study indicates that to maintain high efficiency and purity for this analysis good hadronic energy resolution ($<$20% / $\sqrt{E_{had}}$) and angular resolution are required. In addition, good particle ID by dE/dx is crucial to distinguish protons which interact from pions.

2.3.4 A-dependence of the coherent cross-section

Another task for MINERνA will be comparison of reaction rates for lead and carbon. The expected yield from lead will be $\approx$ 1800 charged-current events, assuming the same efficiency. The A-dependence of the cross-section depends mainly on the model assumed for the hadron–nucleus interaction, and serves as a crucial test for that component of the predictions. No experiment to date has been able to perform this comparison. For reference, the predicted ratio of carbon to lead neutral-current cross-sections at 10 GeV in the Rein-Sehgal and Paschos models are 0.223 and 0.259, respectively [6]. Figure 2 shows the predicted A-dependence according to the model of Rein and Sehgal.

2.3.5 Neutral-current cross-section

Neutral-current π^0 production can occur through a number of mechanisms - resonant production, coherent production, and deep-inelastic scattering. Figure 4 shows a striking example of MINERνA's response to coherent π^0 production.

By requiring two well-separated electromagnetic clusters that shower in the scintillator target, and extend at least 6 scintillator planes, about 30% of the coherent π^0 events produced in the detector are retained. Furthermore, by requiring the ratio of the energy in the two clusters to that of the total event

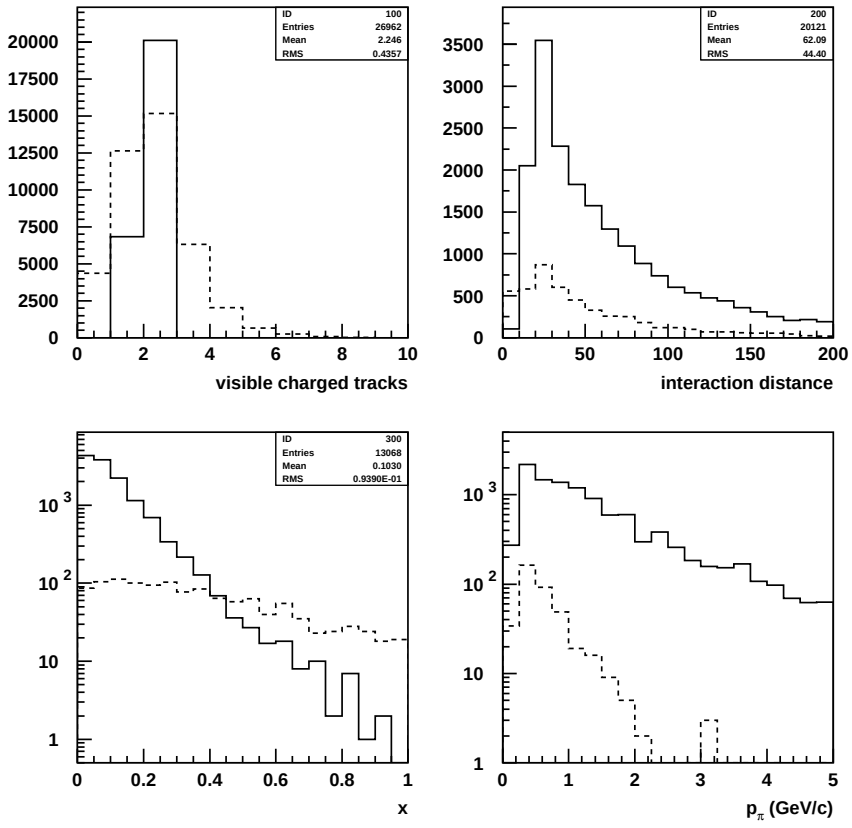

Figure 1: Topological and kinematic quantities for signal (solid) and background (dashed) processes. Top Left: Visible charged tracks. Top Right: Distance between the event vertex and the location of the pion interaction (in cm). Bottom Left: Bjorken-x. Bottom Right: Charged pion momentum.

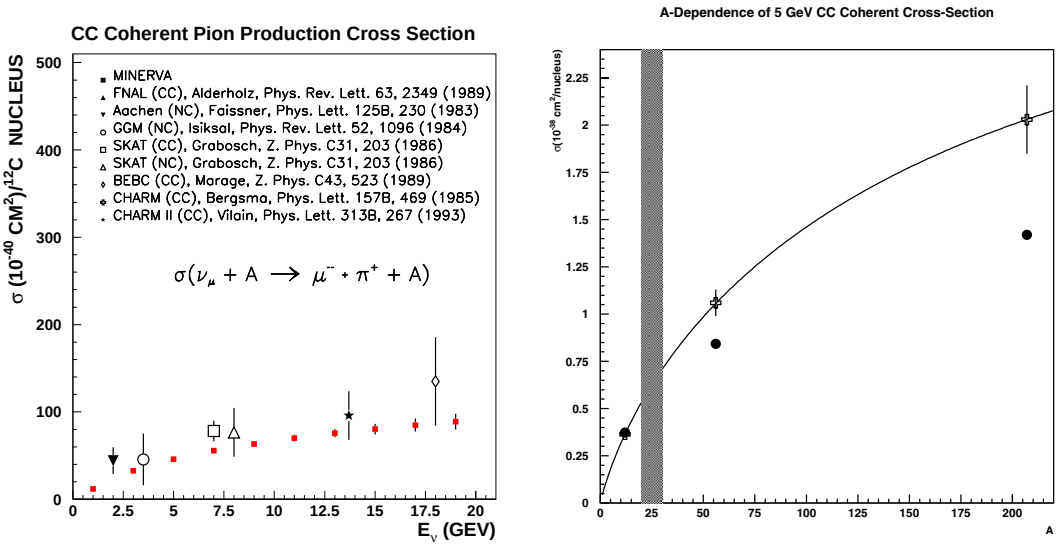

Figure 2: Left: Coherent cross-sections measured by MINERνA compared with existing published results. MINERνA errors here are statistical only. Right: Measurement of the coherent cross-section as a function of atomic number in MINERνAThe shaded band indicates the range of previous measurements. Error bars indicate the size of the experimental errors in a single 1-GeV bin. The curve shows the prediction from the Rein-Seghal model. Crosses are the prediction of the Rein-Seghal model for scattering from carbon, iron, and lead, circles are the predictions of the Paschos-Kartavtsev model.

energy to be above 90%, and requiring any extra energy to be less than 100 MeV, reduces both the ν_e (ν_μ) charged-current contamination to a few (less than one) events. Figure 5 shows these two last variables, where the coherent π^0 peak is clearly visible in the plot on the right. The resulting sample in this simple analysis (1000 events per year in 3 tons of fiducial mass) is roughly half resonant π^0 production and half coherent π^0 events, which can be separated by studying the angular and energy distribution of the events, as well as the presence or absence of additional particles at the production vertex identified by the two photon showers.

Neutral pions from resonance excitation are neither as energetic nor as collinear as those produced coherently. Resonant π^0 are particularly susceptible to final-state nuclear interaction and rescattering, which will be studied in detail by MINERνA using charged-current reactions.

As a proof-of-concept, a sample of neutral-current single-π^0 events has been selected using simple cuts. For events with two well-separated electromagnetic clusters ($E_\pi \equiv E_1 + E_2$), each passing through at least six planes of the fully-active region, requiring $E_\pi/E_{tot} > 90\%$ and $E_{tot} - E_\pi < 100$ MeV efficiently isolates a neutral-current π^0 sample, as shown in Figure 6. After these cuts, the contamination of ν_e and ν_μ charged-current interactions (combined) is less than 1%. The resulting sample contains about 2400 neutral-current π^0 events per 3 ton-yr, of which half are resonant and half coherent.

Coherent and resonant interactions can be cleanly separated by cutting on the π^0 angle to the beam direction, as shown in Figure 7, which also highlights MINERνA's excellent π^0 angular resolution. The overall efficiency for selecting coherent neutral-current π^0 is about 40%.

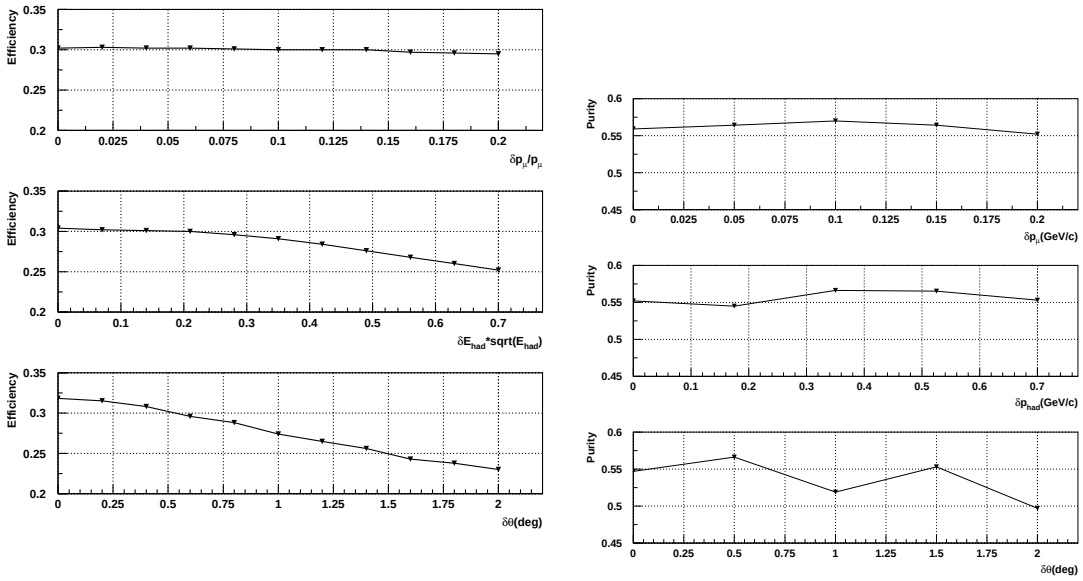

Figure 3: Left: Efficiency of CC coherent selection as a function of angular resolution, muon energy resolution, and hadronic energy resolution. Right: Purity of CC coherent selection as a function of the same variables. Note that in the hadronic energy resolution plots the x-axis is the coefficient of the $1/\sqrt{E_{had}}$ term.

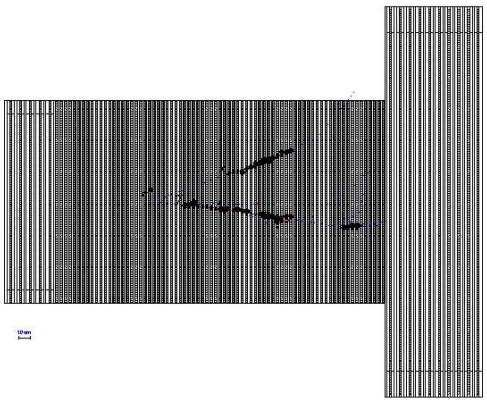

Figure 4: A simulated neutral-current coherent π^0 production event in MINERνA. The position of the π^0 decay vertex can be determined accurately by extrapolating the two photons backward. Notice that both photons pass through a number of planes before beginning to shower, distinguishing them from electrons.

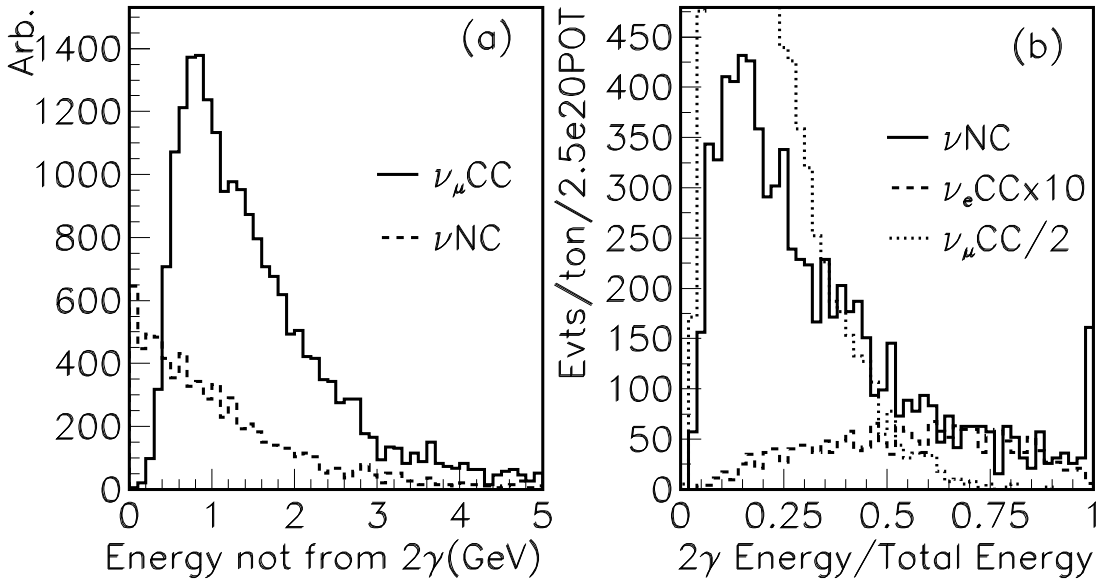

Figure 5: Variables that reject backgrounds to coherent π^0 measurements: (a) Other energy in the event for ν_μ charged- and neutral-current events, and (b) Ratio of two photon energy to total event energy for ν_μ charged-current sample (reduced by factor of 2), ν_e charged-current (increased by a factor of 10) and the neutral-current sample (normalized per ton per year, acceptance calculated for 3 tons fiducial volume)

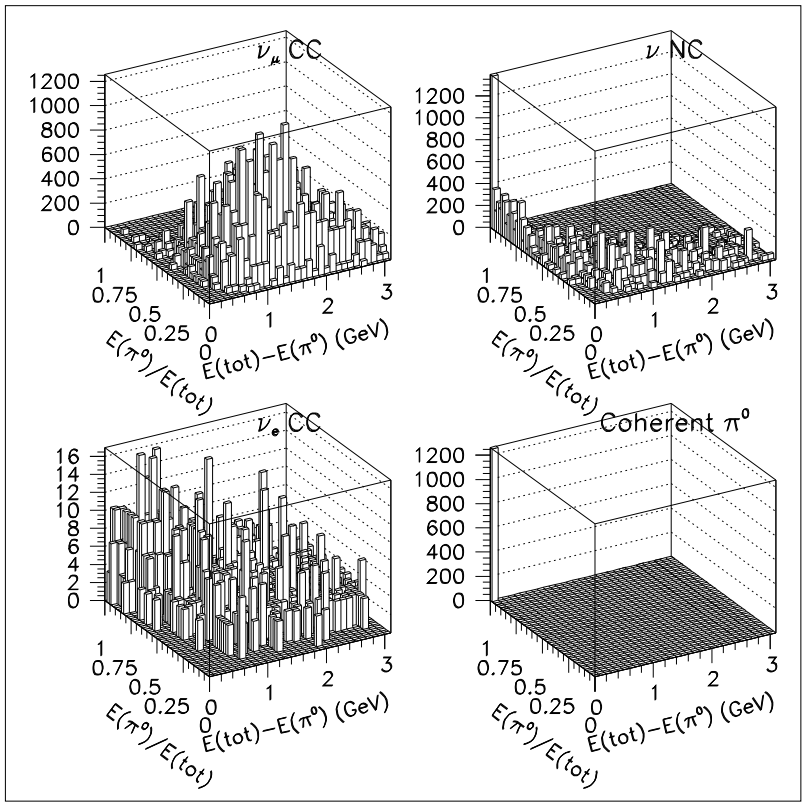

Figure 6: Selection of neutral-current single-π^0 production. The variables plotted are the fraction of visible energy carried by the π^0 candidate (E_π/E_{tot}) and the residual energy $E_{tot} - E_\pi$. The left-hand plots show backgrounds from ν_μ(top) and ν_e(bottom). The plot at top right shows the same distribution for true neutral-current π^0 production, and the lower right shows the subset from coherent scattering. In the neutral-current plots, notice the dramatic concentration of the coherent π^0 signal in a single bin, in the left-most corner of the graph. All samples shown are normalized to a 3 ton-yr exposure of MINERνA.

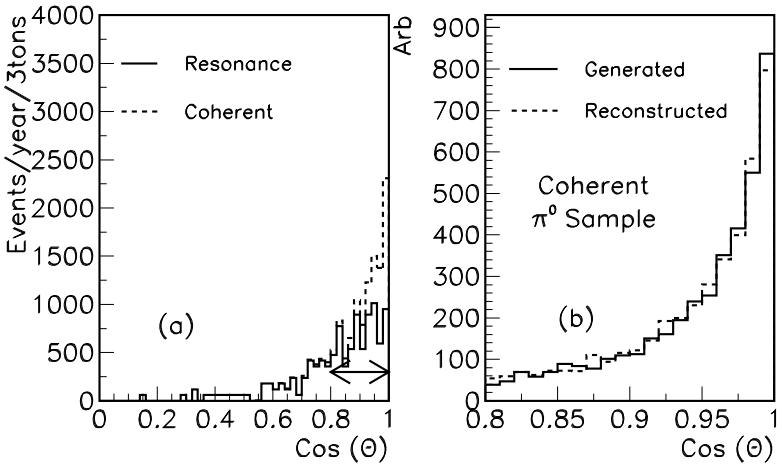

Figure 7: Angular distribution of neutral-current single-π^0 sample. The plot at left shows all events passing the cuts on E_π/E_{tot} and $E_{tot}-E_\pi$ described in the text, broken down into coherent and resonant reactions. The coherent sample is strongly forward-peaked. The plot at right is a close-up of the forward region comparing the true and reconstructed π^0 angular distributions from the beam direction. The distributions are nearly identical, highlighting the MINERνA's excellent angular resolution.

References

[1] D. Rein and L. M. Sehgal, Nucl. Phys. **B223**, 29 (1983).

[2] E. A. Paschos and A. V. Kartavtsev, (2003), hep-ph/0309148.

[3] Super-Kamiokande and K2K, C. Mauger, Nucl. Phys. Proc. Suppl. **112**, 146 (2002).

[4] BooNE, J. L. Raaf, Nucl. Phys. Proc. Suppl. **139**, 47 (2005), hep-ex/0408015.

[5] B. Z. Kopeliovich, Nucl. Phys. Proc. Suppl. **139**, 219 (2005), hep-ph/0409079.

[6] E. A. Paschos, A. Kartavtsev, and G. J. Gounaris, (2005), hep-ph/0512139.

[7] D. Rein and L. M. Sehgal, (2006), hep-ph/0606185.

[8] S. K. Singh, M. Sajjad Athar, and S. Ahmad, (2006), nucl-th/0601045.

[9] MiniBooNE, J. Monroe, Nucl. Phys. Proc. Suppl. **139**, 59 (2005), hep-ex/0408019.

[10] K2K, T. Ishida, Prepared for 1st Workshop on Neutrino - Nucleus Interactions in the Few GeV Region (NuInt01), Tsukuba, Japan, 13-16 Dec 2001.